

Strength of sandy and clayey soils cemented with single and double fluid jet grouting

Modoni Giuseppe^{a,*}, Wanik Lidia^b, Mascolo Maria Cristina^a, Salvatore Erminio^a
Bzówka Joanna^b, Shen Shui-Long^c, Daniele Valeria^d, Pingue Luca^e

^a University of Cassino and Southern Lazio, via di Biasio 43, 03043 Cassino, FR, Italy

^b Silesian University of Technology, Akademicka 5, 44-100 Gliwice, Poland

^c Jiao Tong University, 800 Dong Chuan Rd., Shanghai 200240, China

^d University of L'Aquila, Piazzale E. Pontieri 1, 67100 Monteluco di Roio, L'Aquila, AQ, Italy

^e TREVI s.p.a., Via Dismano, 5819, 47522 Cesena, Italy

Received 3 October 2018; received in revised form 15 March 2019; accepted 28 March 2019

Abstract

Innovations in jet grouting technology have primarily focused on the cutting efficiency of the jets, with the aim of creating larger columns and increasing the productivity of construction sites. Relatively little attention has been paid to the consequences of the grouting system on the mechanical properties of the formed material. This paper investigates this aspect by analysing the results of two field trials carried out in both sandy and clayey soils, where single and double fluid jet grouting were simultaneously performed, with varied grout composition and injection parameters. Parallel uniaxial compressive tests on samples cored from the columns show that the material formed with the double system is systematically lower in strength than the material formed using the single fluid system. The mineralogical composition of samples cored from the columns was analysed by performing parallel Scanning Electron Microscopy (SEM), X-ray diffraction analysis (XRD), Differential Thermal Analysis (DTA) and Thermo-Gravimetric Analyses (TGA) to determine the reasons for this difference. A lower proportion of cementitious products, an accelerated carbonation of portlandite and a less homogeneous distribution of cement hydration products was found on the surface of the soil particles of the double samples than for the single fluid columns.

© 2019 Production and hosting by Elsevier B.V. on behalf of The Japanese Geotechnical Society.

Keywords: Jet grouting; Uniaxial compressive strength; Sand; Clay; Mineralogy

1. Introduction

From its earliest application (e.g. Miki, 1973), jet grouting has greatly progressed (e.g. Croce et al., 2014) and now competes with other engineering solutions in many

geotechnical applications ranging from foundation reinforcement (Modoni and Bzówka, 2012), impervious walls (Croce and Modoni, 2007), bottom plugs (Modoni et al., 2016a), and tunnels (Ochmański et al., 2015a; Qiu et al., 2018; Atangana Njock et al., 2018a). The basic principle of the technology is to form columns of cemented material in situ, mixing the soil with high speed jets of water-cement grout. With time, the challenge became to increase the pumping power and the hydrodynamic efficiency of the injection systems in order to make the technology more productive, increasing the size of columns and consequently reduce the time required for their installation.

Peer review under responsibility of The Japanese Geotechnical Society.

* Corresponding author.

E-mail addresses: modoni@unicas.it (G. Modoni), lidia.wanik@polsl.pl (L. Wanik), mc.mascolo@unicas.it (C. Mascolo Maria), e.salvatore@unicas.it (E. Salvatore), joanna.bzowka@polsl.pl (J. Bzówka), slshen@sjtu.edu.cn (S. Shui-Long), valeria.daniele@univaq.it (V. Daniele), lpingue@trevispa.com (L. Pingue).

<https://doi.org/10.1016/j.sandf.2019.03.007>

0038-0806/© 2019 Production and hosting by Elsevier B.V. on behalf of The Japanese Geotechnical Society.

Nowadays, columns with diameters as large as three meters and more are possible (Eramo et al., 2012). In addition, the most recent equipment makes it possible to selectively control the rotating speed of the monitor and create columns of non-circular sections (e.g. elliptical, rectangular, square), which is particularly convenient when irregular volumes must be covered (e.g. Flora et al., 2017). Notably, the innovations have resulted in a marked reduction in the number of boreholes and in the time needed to create massive structures like bottom plugs or cut-off walls. The larger efficiency of the cutting systems has considerable environmental benefits as well, since a lower amount of spoil is produced. In this race, one of the most effective technological innovations is represented by the so-called double-fluid jet grouting. This injection system consists of two coaxial jets, an internal jet of massive fluid, which aims at eroding the soil, an outer annular jet of air which functions to coat the inner one and protect it against the turbulent exchange of forces and mass with the material filling the space outside the nozzle (Modoni et al., 2006; 2016b; Flora et al., 2013, Ochmański et al., 2015b, Shen et al., 2013). This principle is also at the base of the triple fluid system, where an air-assisted water jet is firstly injected to cut the soil and a second jet of cement grout follows to provide cementation. Nowadays, the possibility of getting higher pumping pressures and flow rates has made the double fluid system the most popular, with applied energies as high as 1400% above the first application (see Fig. 1). This system is considered effective in almost all soil types, even those particularly resistant to cutting.

While there is much concern about the dimensions of columns, little attention is paid to the consequence of the injection system on the mechanical properties of the jet-grouted material. This situation basically is basically due to the overabundanc of jet grouted structures and their provisional functions. That is, high strength is generally not a paramount requirement. Nonetheless, more accurate

control of the mechanical properties of the material based on a deeper knowledge of their relationship with the executive factors may increase confidence in this technology, optimize its use and, perhaps, pave the way to assigning a permanent function to jet grouted structures.

Studies performed on samples of cement stabilised clayey soil carefully reconstituted in the laboratory with variable composition (e.g. Lee et al., 2005; Kitazume and Terashi, 2013; Atangana Njock et al., 2018b) contribute to quantify the influence of constituent materials (water, cement and soil) and their relative proportions on the strength of cemented soil. Atangana Njock et al. (2018b) noted a noticeable reduction of the uniaxial compressive strength with the water-cement ratio of the mix, confirming previous results from Kaushinger et al. (1992). Lee et al. (2005) also found a slight decrease in the cement-soil ratio. This apparently surprising result is motivated by the authors with a more flocculated and porous structure of the clayey material containing a higher fraction of cement.

Kitazume and Terashi (2013) have provided a comprehensive classification of the factors influencing the chemical reaction between soil and binder (here reported in Table 1). For a complete overview of the dependency of the uniaxial compressive strength on each factor, readers may refer to their original publication. It must, however, be pointed out that the above studies consider clayey soils, and the results therefore cannot be extended to non-plastic materials (e.g. sand) treated with jet grouting.

In considering the objective of the present study, i.e. the role of jet grouting injection system, many of the factors listed in Table 1 are independent on the technology. Those which might vary between single and double fluid injection systems, and thus deserve to be carefully analysed, have been marked with an asterisk. Even when the injection parameters are assigned and measured, the composition of jet grouting material cannot be known with a good accuracy, and some uncertainty will always exist. This is

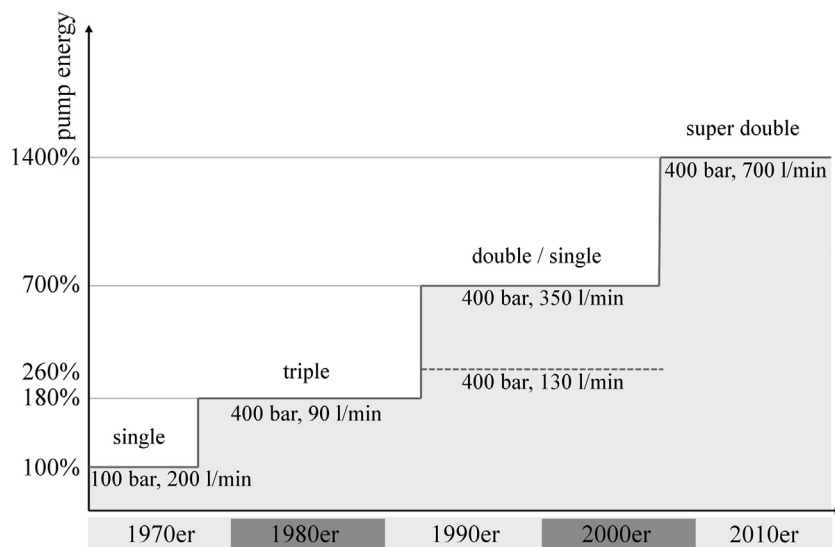


Fig. 1. Time evolution in the use of jet grouting (from Flora et al., 2017).

Table 1

Factors affecting strength increase of cement stabilised soil (derived from Kitazume and Terashi, 2013).

I. Characteristics of binder	1. Type of binder 2. Quality 3. 3. Mixing water and additives (*)
II. Characteristics and conditions of soil	1. Physical, chemical and mineralogical properties of soil (especially for clays) 2. Organic content 3. Potential Hydrogen (<i>pH</i>) of pore water 4. 4. Water content
III. Mixing conditions	1. Degree of mixing (*) 2. Timing of mixing/re-mixing 3. 3. Quantity of binder (*)
IV. Curing conditions	1. Temperature 2. Curing period 3. Humidity 4. Wetting and drying/freezing and thawing, <i>etc.</i> 5. Overburden pressure

(*) Parameters likely to be influenced by the jet grouting injection system

because the formation of the column is ruled by factors controllable up to a limited extent, primarily the variability in the soil composition and the imperfect mixing with grout. One of the most evident effects is the considerable heterogeneity of the material that results in variation coefficients of the uniaxial compressive strength as high as 70% (Toraldó et al., 2018). However, despite this variability, the few studies attempting to quantify the role of the injection system (*e.g.* Van der Stoel, 2001) have reported a systematically lower strength of material created with the double fluid system than that created with the single fluid (Fig. 2). A strong dependency on the injection system is also envisaged by Tinoco et al. (2014) who carried out a

systematic collection and interpretation with advanced statistical methods (Support Vector Machines) of field data from different jet grouting projects. Considering all the possible factors, these authors found the injection system to have the second highest relative importance on the unconfined compressive strength of the produced material, the first being the ratio between porosity and cement content of the material. Considering also that porosity and cement content of the material are both influenced by the injection system, it is evident that the technology deserves to be investigated with more attention.

Starting from these premises, the present study interprets the influence of the injection system on the mechanical properties of jet grouted material from a micromechanical perspective. To this aim, classical mechanical tests have been coupled with microscopic observation and thermo-physical tests to investigate the mineralogical composition of samples formed in two different soil types (cohesive and cohesionless) with single and double fluid jet grouting.

2. Experimental study

To investigate the dependence of the injection system on the strength of the jet grouted material, two field trials have been performed. In both cases, columns were simultaneously created with single and double fluid jet grouting systems, then their top portions were excavated, and samples were core, taken to the laboratory and investigated with a set of mechanical and chemical tests. Considering that the properties of the jet material depend significantly on the constituent soil (*e.g.* Toraldó et al., 2018), two test sites were selected for the evaluation of the performance of the injection systems in both sandy and clayey deposits.

2.1. Case study #1: Sandy soils

This first field trial was performed in Silesia (Poland) with the general purpose of investigating the effects of

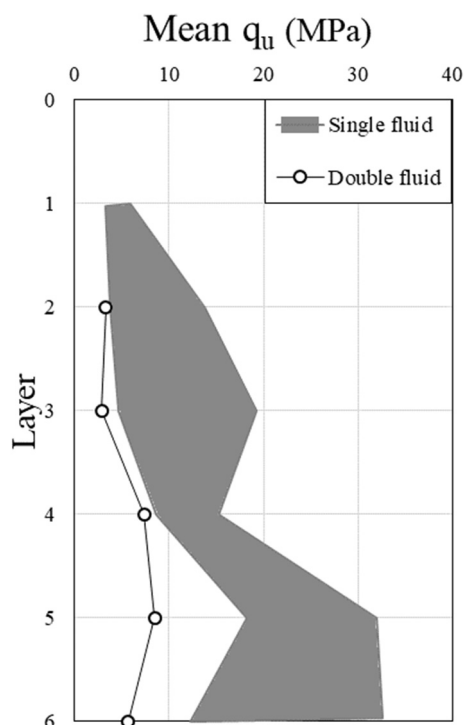


Fig. 2. Strength of jet grouted columns created in the same soil with single and double fluid jet grouting (adapted from Van der Stoel, 2001).

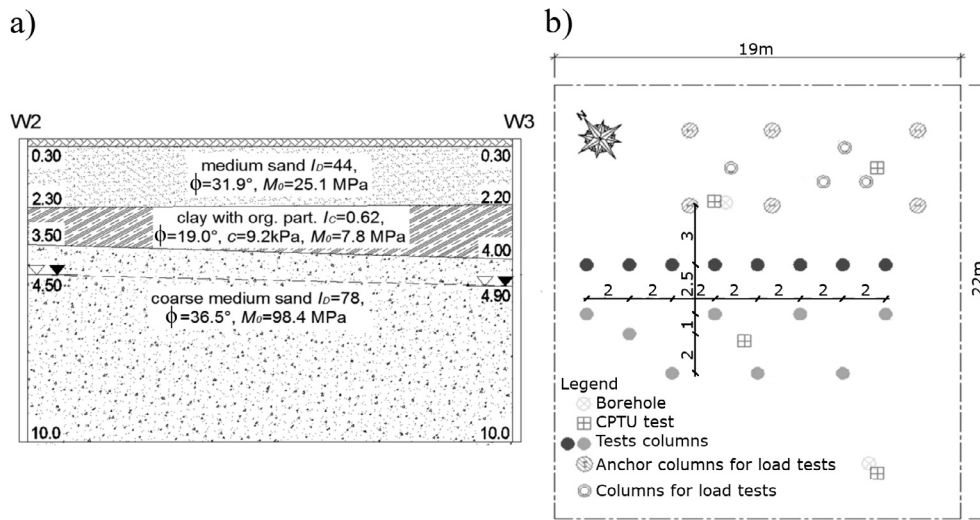


Fig. 3. Field trial in sandy soils: stratigraphy of the subsoil (a) and layout of columns (b) (Wanik, 2017).

injection systems and parameters on the diameter and mechanical properties of columns (Wanik, 2017; Wanik et al., 2017). The subsoil stratigraphy was investigated with two boreholes and four Piezocone Tests (CPTU) to determine the alluvial sequence shown in Fig. 3a, with a top layer of medium sand superposed to organic clays and coarse sand. Sixteen columns of about 4 m in length (from about 0.5 m to 4.5 m below ground level) were created, eight with single fluid and eight with double fluid system (indicated respectively as 1S–8S and 1D–8D in Fig. 3b). The same lifting speed was assigned to all columns, while the flow rate was modified by parametrically modifying the diameter of the nozzles and injection pressure (Table 2). The same binder type, Portland composite cement mixed with fly ash (code CEM II/B-V 32.5 R - EN 197-1, 2011), and cement-water (equal to 1) were used for all columns.

Columns were then excavated up to 1.5 m depth below the ground surface (Fig. 4a) to measure the diameters and to take core samples representative of the material (see Fig. 4b).

The mean diameters of the single and double fluid jet grouting columns, reported in Table 2 together with the injection parameters, show a clear dependency on the grout flow rate. Although important, this issue is out of the scope of the present work. Here, it is just important to note that the columns created with double fluid had larger dimensions than those formed with the single fluid system.

2.1.1. Uniaxial compressive tests

Several samples were extracted from the top portion of the columns, *i.e.* the one formed in the medium sand layer (see Fig. 4b), and were taken to the laboratory and subjected to uniaxial compression tests. The results, also reported in Table 2, show the differences between the materials created with single and double fluid. The statistical analysis of these data, summarized in Table 3, shows some limited relevance to the slenderness of the samples, as the

tests performed on specimens with a height to diameter ratio (h/d) equal to one or two give comparable results. On the other hand, there is a very strong influence on the injection systems as the measured Uniaxial Compressive Strength (q_u) range between 11.7 and 11.8 MPa for the single fluid material, between 1.1 and 3.2 MPa for the double fluid system, *i.e.* the strength is from 365 to 1000% higher for the single than for the double fluid. Such a difference cannot be explained by the higher presence of voids in the double fluid material (induced in principle by the injection of air), as the dry unit weight of the two materials (single and double fluid) is similar (see Table 3).

Therefore, an attempt has been made to correlate the variation of strength seen in Table 2 with the composition of the materials with particular attention to the amount of cement in relation to water and soil. In fact, as the adopted parameters (namely grout composition and flow rates, lifting speed of the monitor) are similar for the two injection systems and the diameter larger for the double fluid columns, a lower presence of cement must be assumed for the second case. To quantify this effect, the cement content in each column has been calculated starting from the composition of grout (cement–water ratio was equal to 1 in all cases), the injected flow rate, the lifting speed of the monitor and the diameter of the columns (Table 2). Water-cement and cement-soil ratios have been estimated assuming an initial porosity of the soil equal to 0.3 and equal composition for the material present in the column and in the spoil. It should be noted that because it is not possible to retrieve and quantify the amount of cement directly from samples, indirect estimates were made. These estimates affect the absolute values of the quantities computed in Table 2, but certainly do not alter the relative conditions between single and double fluid material.

The computed values are reported in Table 2 and plotted against uniaxial compressive strength in Fig. 5. Despite some unavoidable scattering, the position of the two

Table 2
Injection parameters and fundamental properties of the different columns of the field trial performed in sandy soils (Wanik, 2017).

Column #	Nr and diameter [mm] of nozzles	GROUT pressure [MPa]	GROUT flow rate [m ³ /s]	Lifting speed [m/s]	Mean diameter [m]	Cement per unit volume of column [kg/m ³]	Cement-soil ratio	Water-cement ratio	Mean uniaxial compressive strength [Mpa]
1S	2x4.0	36	0.0053	0.0083	1.13	291	0.61	1.63	7.80
2S	2x2.8	36	0.0026	0.0083	0.94	232	0.43	1.89	4.55
3S	2x4.0	18	0.0037	0.0083	0.9	310	0.68	1.57	20.80
4S	2x2.8	25	0.0022	0.0083	0.78	264	0.52	1.74	
5S	2x4.0	36	0.0053	0.0083	1.13	291	0.61	1.63	11.60
6S	2x2.8	36	0.0026	0.0083	0.98	219	0.40	1.97	11.08
7S	2x4.0	18	0.0037	0.0083	0.9	310	0.68	1.57	11.31
8S	2x2.8	25	0.0022	0.0083	0.86	231	0.43	1.90	11.07
1D	2x4.0	36	0.0053	0.0083	1.75	157	0.25	2.52	
2D	2x4.0	18	0.0037	0.0083	1.61	135	0.21	2.82	1.60
3D	2x4.0	36	0.0053	0.0083	1.73	159	0.26	2.48	3.40
4D	2x4.0	18	0.0037	0.0083	1.58	139	0.22	2.75	3.10
5D	2x2.8	36	0.0026	0.0083	1.54	107	0.16	3.39	3.30
6D	2x2.8	26	0.0022	0.0083	-				1.60
7D	2x2.8	36	0.0026	0.0083	1.88	76	0.11	4.57	5.30
8D	2x2.8	25	0.0022	0.0083	1.63	83	0.12	4.22	1.30

families of dots reveals a clear correlation between the adopted variables, and their relative position justifies the different uniaxial compression strength. The dependency on the water-cement ratio is in complete accordance with the results provided by Atangana Njock et al. (2018a, 2018b) and Lee et al. (2005), while the dependency on the cement-soil ratio follows an opposite trend. However, it must not be forgotten that the present tests have been conducted in sandy soils (Iolli et al., 2015; Salvatore et al., 2017), whereas Lee et al. (2005) refer to clayey soils which are characterized by different chemical reactions with cement. Fig. 5b shows that the uniaxial compressive strength increases significantly with the cement/soil ratio and this result suggests it is possible to accurately control the amount of injected cement considering the size of columns produced with each technology.

2.1.2. Mineralogical composition

The role of the injection system was investigated by a series of laboratory tests, using small pieces of material from the tested samples to get a deeper insight in the mineralogical composition of the two materials. An immediate confirmation of the different presence of cement in the material for single and double fluid system is seen from the Scanning Electron Microscope (SEM, Reimer, 1998) analysis, whose typical results are reported in Fig. 6. In fact, the sample treated with single fluid (Fig. 6a) shows a diffused presence of plate-like portlandite crystals aggregates (Mascolo et al., 2010) and calcium silicate hydrate particles (CSH) surrounding the bigger quartz grains. These minerals, scarcely present in the double fluid material (Fig. 6b), are produced from the hydration of cement and are the main reason for the binding action, and therefore, the biggest contributors to the material strength (Taylor, 1997).

Along with natural soil directly taken from the test site, the two samples of material created with single and double fluid were subjected to X-ray diffraction (XRD, Klug and Alexander, 1974), differential thermal (DTA, MacKenzie, 1970) and thermogravimetric analyses (TGA, Coats and Redfern, 1963). The XRD technique allowed the crystalline composition of the materials to be characterized. The typical pattern (Fig. 7) shows several peaks, each produced by the constructive interference of a monochromatic beam of X-rays diffracted at specific angles from a set of lattice planes in the crystalline structure of the material. The intensities of each peak are determined by the distribution of atoms within the crystalline lattice. Consequently, the X-ray diffraction pattern is the fingerprint of the periodic atomic arrangements in a given material structure. To identify the different components, the observed diffraction peaks are compared with an official database of the International Centre for Diffraction Data (ICDD, 2017) associating each angle to a specific crystalline phase.

The XRD pattern of the natural soil (Fig. 7a) reveals that quartz, SiO₂, (JPCDS card no. 46-1045) is the prevalent crystalline phase of the sand and that dolomite

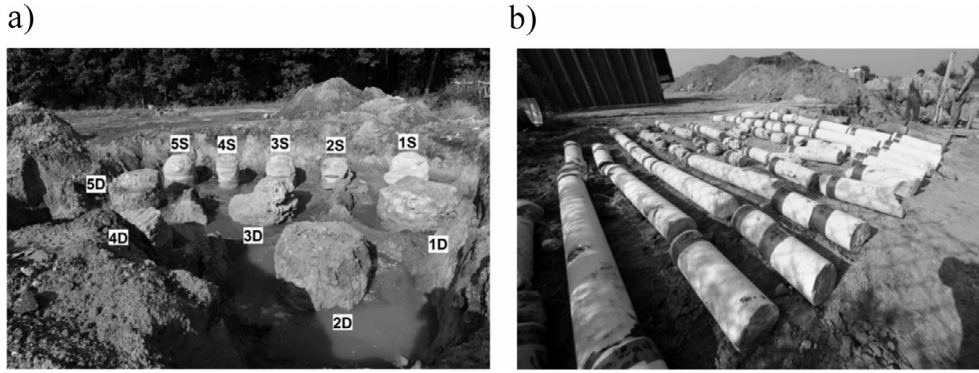


Fig. 4. Top of the excavated columns (a) and cored samples (b) (Wanik, 2017).

Table 3
Statistics of the different laboratory tests performed on the material coming from the field trial in sandy soils.

Shape ratio h/d	h/d = 1.0		h/d = 2.0	
	Single	Double	Single	Double
Jet grouting system				
Number of samples	22.0	15.0	19.0	8.0
Mean dry unit weight [kN/m ³]	16.5	16.9	16.9	17.4
Standard deviation unit weight [kN/m ³]	1.2	1.0	1.9	0.5
Mean q _u [MPa]	11.7	3.2	11.8	1.1
Standard deviation q _u [MPa]	1.6	0.5	1.1	0.1

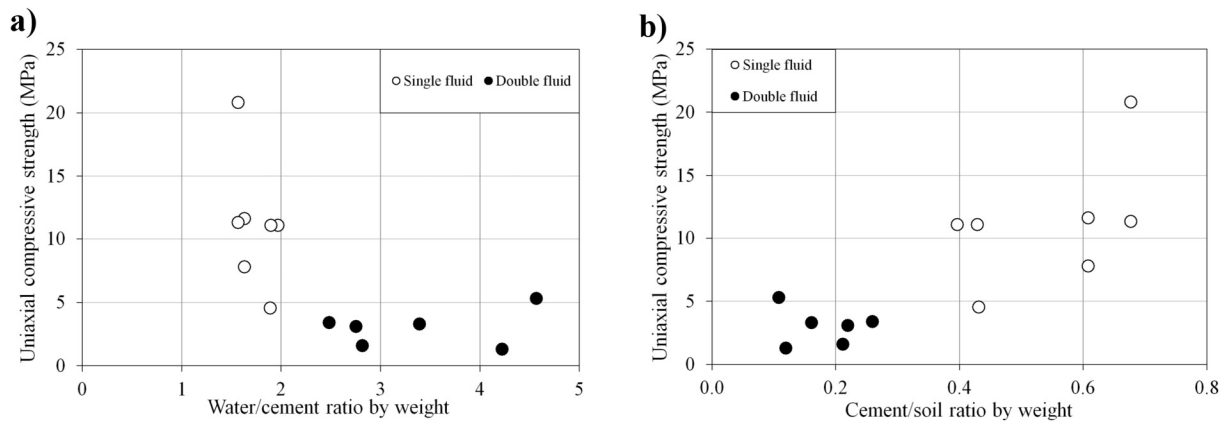


Fig. 5. Dependency of the uniaxial compressive strength on the estimated water-cement (a) and cement-soil (b) ratios of the jet grouted material.

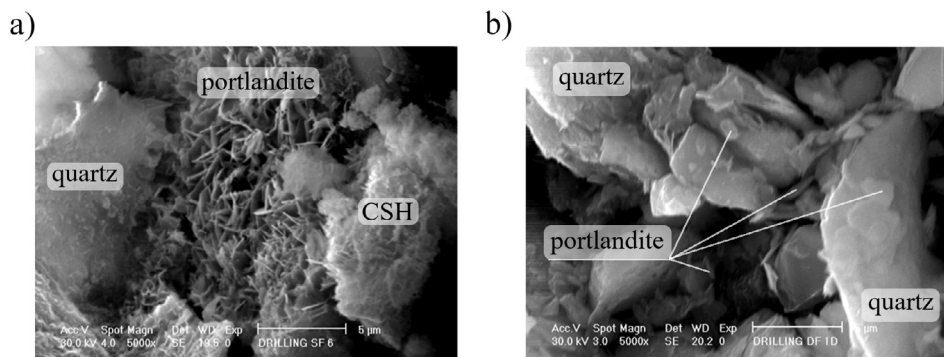


Fig. 6. SEM micrographs of samples treated with single (a) or double (b) fluid system.

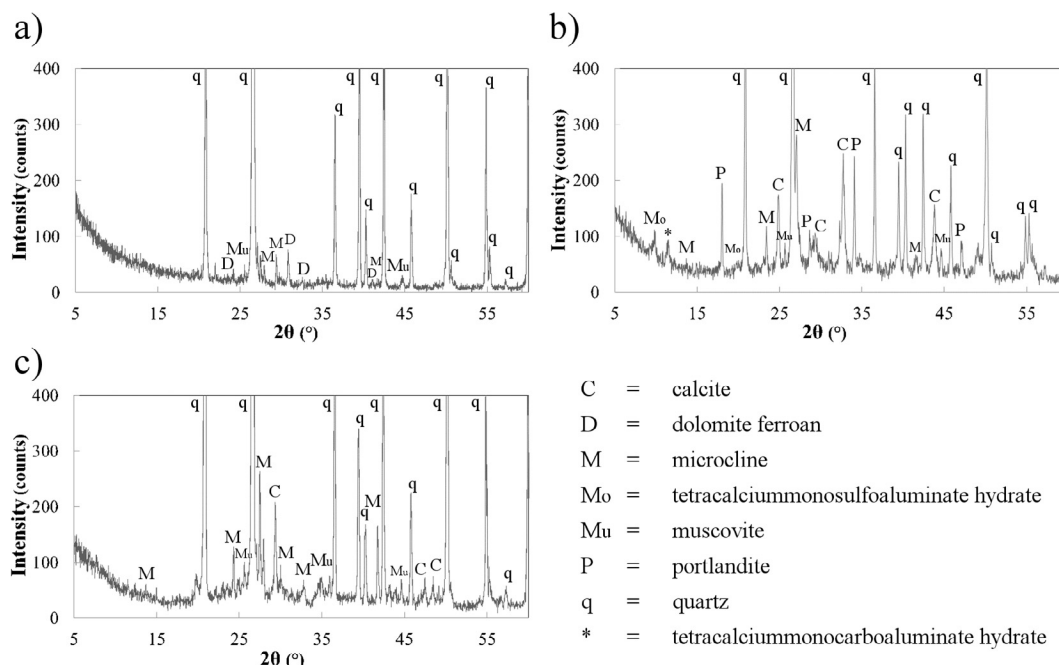


Fig. 7. XRD patterns of the natural soil (a), of the soil treated with single (b) and double (c) fluid jet grouting.

ferroan, $\text{Ca}(\text{Mg}, \text{Fe})(\text{CO}_3)_2$, (JPCDS card no. 34-517), muscovite, $\text{KAl}_3\text{Si}_3\text{O}_{10}(\text{OH})_2$, (JPCDS card no. 1-1098) and microcline, KAlSi_3O_8 , (JPCDS card no. 19-932), are present with progressively lower amounts. The same test performed on soil treated with single fluid jet grouting (Fig. 7b) reveals the presence of the above components together with portlandite $\text{Ca}(\text{OH})_2$, (JPCDS card no. 44-1481), calcite, CaCO_3 , (JPCDS card no. 13-192), tetracalcium monosulfoaluminate hydrate, $3\text{CaO}\cdot\text{Al}_2\text{O}_3\cdot\text{CaSO}_4\cdot x\text{H}_2\text{O}$, (JPCDS card no. 18-275), and tetracalcium monocarboaluminate hydrate, $3\text{CaO}\cdot\text{Al}_2\text{O}_3\cdot\text{CaCO}_3\cdot x\text{H}_2\text{O}$. Portlandite and calcite are typical hydration products of cement, and tetracalciummonocarboaluminate hydrate is formed at early age of cement hydration in presence of limestone or dolomite, while the tetracalciummonosulfoaluminate hydrate is a result of the transformation of ettringite. All these components indicate a meaningful presence of cement.

The comparison with the material created with double fluid jet grouting (Fig. 7c) soil reveals a smaller presence of calcite, while most of the other phases produced by cement hydration are negligible or totally missing.

Another relative effect seen from the XRD test on the materials created with single and double fluid jet grouting can be seen from the results in Fig. 8. Here the peaks are at 26.7° , the diffraction angle typical of quartz are plotted for the materials created with single and double fluid jet grouting. The higher intensity observed for the double fluid material confirms a higher relative presence of quartz minerals than the hydration products of cement.

The original soil and the materials formed by the two injection systems were then subjected to Thermo-Gravimetric (TGA) and Differential Thermal Analyses (DTA) (Fig. 9). The former test consists in measuring the

change of weight while samples are exposed to progressively increasing temperatures. The latter test, run simultaneously with the previous one, measures the difference in temperature between the sample and an inert reference material while the temperature of the room is increased. The peaks of this variable indicate that a chemical-physical transformation, whether endothermic or exothermic, takes place at different temperatures in the sample. The parallel observation of these two analyses (the peaks of the DTA correspondent to the larger decays of TGA) provides information on the different components present in the tested material.

In the present study, the DTA plot of the original soil (Fig. 9a) shows three endothermic peaks at 571.5 , 760.5 and 867.4°C , respectively, for the first representative of the displacive and polymorphic transformation of the quartz, the second and third coming from the

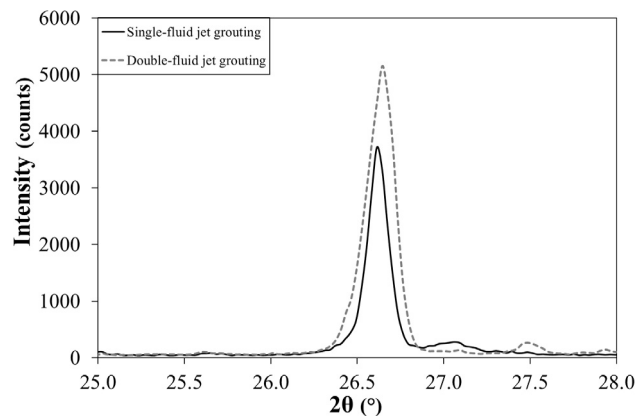


Fig. 8. Main XRD peak of quartz for the soil treated with single and double jet grouting.

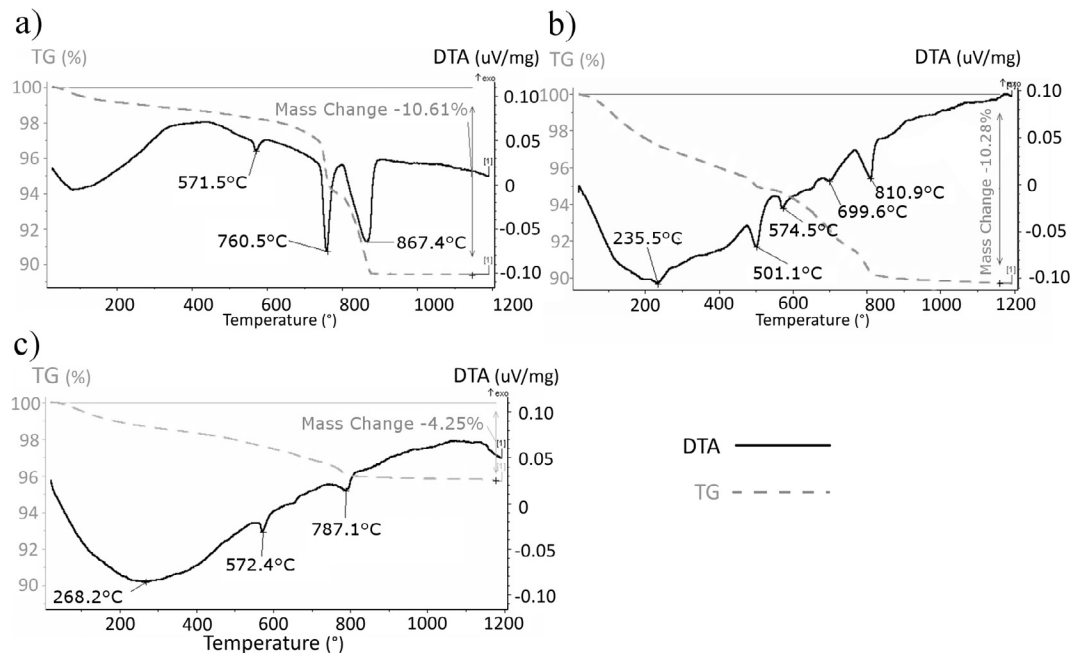


Fig. 9. DTA and TGA of natural soil (a) and of the soil treated with single (b) and double (c) jet grouting.

decomposition of dolomite (MacKenzie, 1970). The same test on the material treated with single fluid jet grouting also shows peaks at 574, 700 and 811 °C, indicative of the transformation of quartz and dolomite. The transformation of dolomite at lower temperatures than in untreated soil can be explained by the reduction of the dolomite crystal size induced by the reaction with cement.

In addition to the above peaks, the single fluid material shows other less intense endothermic peaks at 235 and 501 °C (Fig. 9b), the former (235 °C) indicative of calcium aluminate hydrate phases, the latter (501 °C) induced by the thermal decomposition of portlandite. On the other hand, the DTA experiments performed on the double fluid material (Fig. 9c) reveal only two endothermic peaks, at 572.5 and 787.1 °C, related with the presence of quartz and dolomite. The peaks previously observed on the single fluid material at 235 and 501 °C, resulting from the decomposition of calcium aluminate hydrate phases and portlandite have disappeared.

The curves obtained from TGA tests, reported in the same plot, show for the natural soil (Fig. 9a) a continuous weight loss of about 2% up to the room temperature up to 700 °C and two more marked weight losses (at 760 and 867 °C) related to the decomposition of $MgCO_3$ and $CaCO_3$ present in the dolomite. As expected, no change in the weight loss results at 571 °C from the polymorphic transformation of quartz. The same test performed on the soil treated with single fluid jet grouting (Fig. 9b) reveals a continuous weight loss of 4% for room temperatures lower than 400 °C. This decay, significantly larger than the one seen on the untreated soil, comes from the dehydration of the calcium silicate hydrate phase (CSH)

during its thermal decomposition, typically occurring at temperatures between 150 and 450 °C. The CSH phase, not easy to be distinguished with XRD because of its very low crystallinity (Hewlett, 2003), is the principal binding agent in cement chemistry (Taylor, 1997). Together with the former effect, there is another evident decay at 501 °C, indicative of the transformation of portlandite. Again, this decay is totally absent in the double fluid material (Fig. 9c), which is as a proof of the limited presence CSH and portlandite.

In conclusion, all the above analyses confirm a much lower presence of cement products in the column treated with double fluid, possibly due to the diffusion of cement in larger volumes, that could explain the lower strength observed for this material from the uniaxial compressive tests.

2.2. Case study #2: Clayey soils

The second field trial was performed in northern Italy, in a layer of fine-grained material (Fig. 10a). The interpretation of cone penetration tests with the Robertson (1990) chart (Fig. 10a) leads to the conclusion that the subsoil consists of clayey and silty materials with variable proportions. Two columns were then purposely created here, one with single fluid adopting a cement-water ratio equal to 0.71, the other with double fluid system adopting a cement/water ratio equal to 0.95. Unlike the previous case study, where the cement content in the single and double fluid columns was not specifically controlled, different composition of grout and injection parameters were adopted in this second case, in an effort to obtain more similar cement

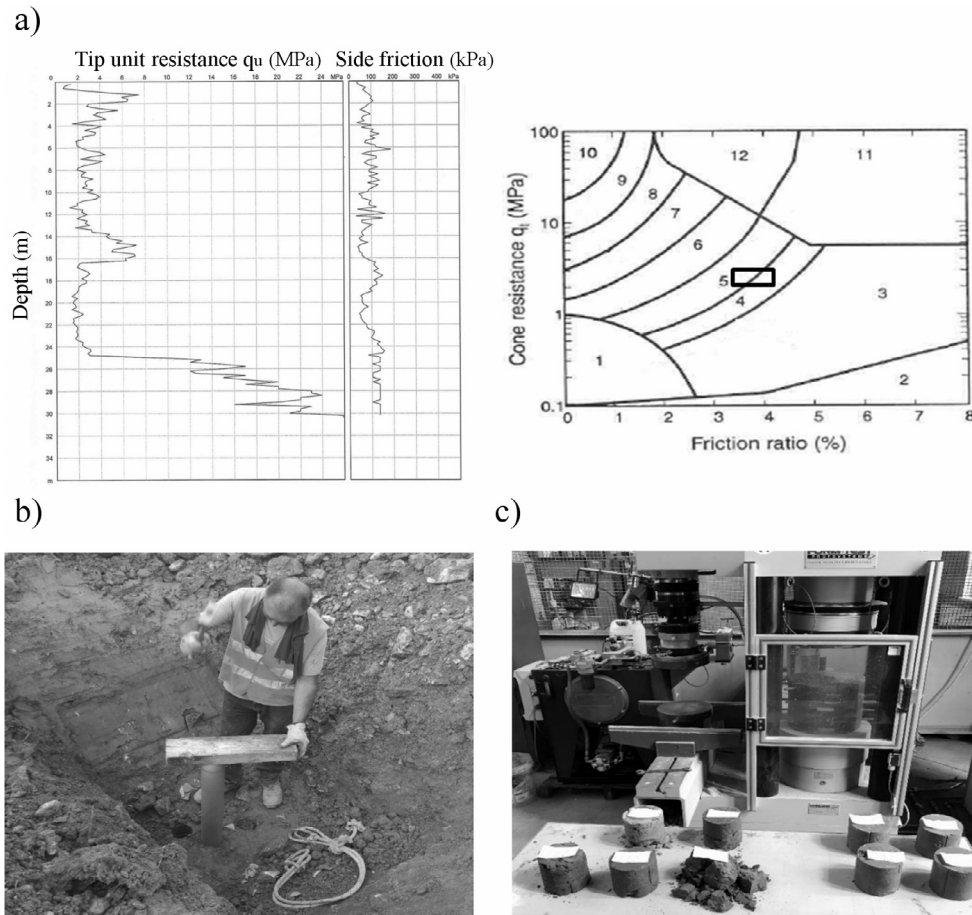


Fig. 10. Field trial in clayey soil (a. CPTU profile and Robertson (1990) chart; b. coring of the sample; c. tested samples and laboratory equipment).

contents for the two columns (see Table 4). In fact, considering the diameter of the two columns, the cement content estimated for double fluid (385 kg/m^3) is slightly higher than for single fluid (353 kg/m^3). As for the previous case study, this calculation has been made assuming an initial porosity of the soil equal to 0.5 and similar composition for jet grouted material and spoil.

After injection, the two columns were excavated in their top meter, samples were cored manually in the fresh jet grouted material (Fig. 10b) and taken to the same laboratory used in the previous case study (Fig. 10c).

Before performing the uniaxial compression tests, the samples were subjected to a series of non-invasive ultrasonic tests consisting in the measurement of the propagation velocities of compressional waves between sources

and receivers placed at various locations on the sample's surface. The complete list of results from these tests, reported in Table 5, shows that the material created with single fluid jet grouting is much stiffer than the one created with the double fluid system. The same conclusion can be derived from the uniaxial compression strength. In all cases, the material strength is particularly low, but while the mean q_u for double fluid is about 150 kPa, the mean strength of single fluid material is 500 kPa (333% higher). It is worth noting that this difference cannot be attributed to the different density of the two materials, even though the dry unit weight of the samples formed with double fluid jet grouting is consistently larger than for the single fluid samples. Neither can the water-cement ratios of the material be invoked to explain the noticed difference, since this

Table 4
Injection parameters and fundamental properties of the different columns of the field trial in clayey soils.

Column #	Nr and diameter [mm] of nozzles	Grout pressure [MPa]	Grout flow rate [m^3/s]	Lifting speed [m/s]	Average diameter [m]	Cement weight per unit volume of column [kg/m^3]	Cement-soil ratio	Water/cement ratio	Average uniaxial compressive strength [MPa]
Single fluid	2x3.5	40	0.0045	0.01	0.6	353	0.71	1.95	0.5
Double fluid	2x3.5	40	0.0044	0.006	0.9	385	0.63	1.66	0.15

Table 5
Results obtained from the different laboratory tests on samples from the field trial in clayey soil.

Injection system	Sample ID	Dry unit weight (kN/m ³)	Mean compressional wave velocity (m/s)	UCS (kPa)
Single	M#1-1	13.3	1055	427
	M#1-2	12.9	961	484
	M#2-1	13.1	1015	569
	M#2-2	13.0	1222	–
Double	B#1-2	14.6	490	–
	B#1-3	16.4	370	175
	B#2-2	15.0	343	122
	B#2-3	15.5	–	–

quantity is larger for the single than for double fluid material. The cement content related to the soil present in the material is slightly larger for single than for double fluid and this could play some role in principle, though it would not be in the same direction as that suggested by Lee et al. (2005), who noticed an opposite dependency. The question needs to be investigated in more detail by looking at the composition of the material.

2.2.1. Mineralogical composition

The SEM analysis at high magnification reveals a meaningful morphological difference between the sample treated with single (Fig. 11a) and double fluid system (Fig. 11b). The two samples show similar particles with dimensions of a few microns, representative of the natural soil. However, while the single fluid material shows the co-existence of sub-microparticles attached to the surfaces of the bigger soil particles, these sub-elements are absent in the double fluid material. These products, coming possibly from the hydration of cement, could be responsible for the greater resistance of the single fluid material. The morphological difference between the two materials, basically occurring from a more homogeneous distribution of the hydration products of cement in the single fluid material, can be justified by a different wettability by the cement suspension with the soil particles. In fact, for the single fluid system, a direct interaction can be assumed between soil particles and cement suspension and hence a single solid-liquid interface. However, because three phases (solid,

liquid and air) are present in the double fluid system (soil particles, liquid cement suspension and injected air), three interfaces should be expected (solid-liquid, solid-air and liquid-air). The increase in the number of interfaces and, particularly the additional presence of the liquid-air and solid-air interfaces, can justify a looser distribution of the binder above the soil particles.

Additionally, the carbonation rate of the portlandite produced by the hydration of cement might play a role. It is well known that a slower carbonation rate results in the growth of bigger calcite crystals in the conglomerate. A faster crystallization rate, like the one induced by the presence of air, may induce the formation of micro tensions resulting in smaller crystals and worsen the mechanical performance of the conglomerate. The insufflation of air carried out in the double fluid system could then have triggered the faster carbonation of the portlandite, and this may explain the reduced strength of the material.

Again, XRD analyses were performed on the different materials, as samples dehydrated in air at 60 °C for 48 h. Fig. 12 shows that single and double fluid treated materials present peaks at similar diffraction angles typical of quartz (q), calcite and clayey components like muscovite and clinchlore. Traces of feldspar and amorphous phases are also found in both materials. Therefore, the differences between the two materials is negligible with regard to the constituent minerals present in the two cases.

Also, simultaneous DTA and TGA (Fig. 13) tests carried out on the two materials show negligible

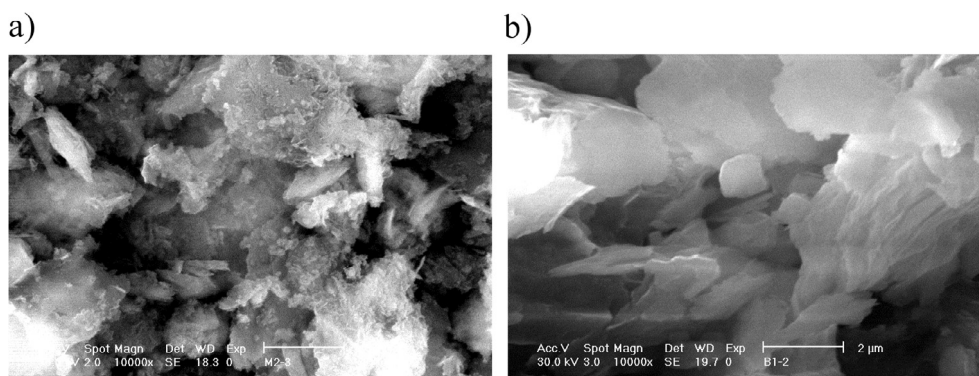


Fig. 11. SEM micrographs of the clayey soil treated with single (a) and double (b) fluid jet grouting.

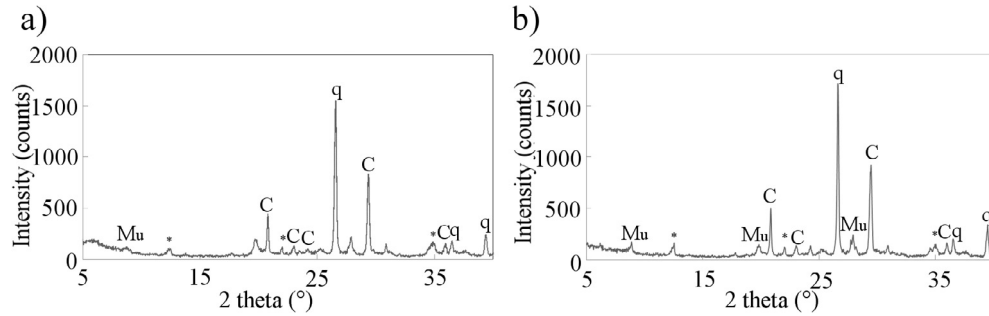


Fig. 12. XRD patterns of the clayey soil treated with single (a) and double (b) fluid jet grouting. (q = quartz; * = clinochlore, $(Mg_5Al)(SiAl)_4O_{10}(OH)_8$; C = calcite, $CaCO_3$; Mu = muscovite).

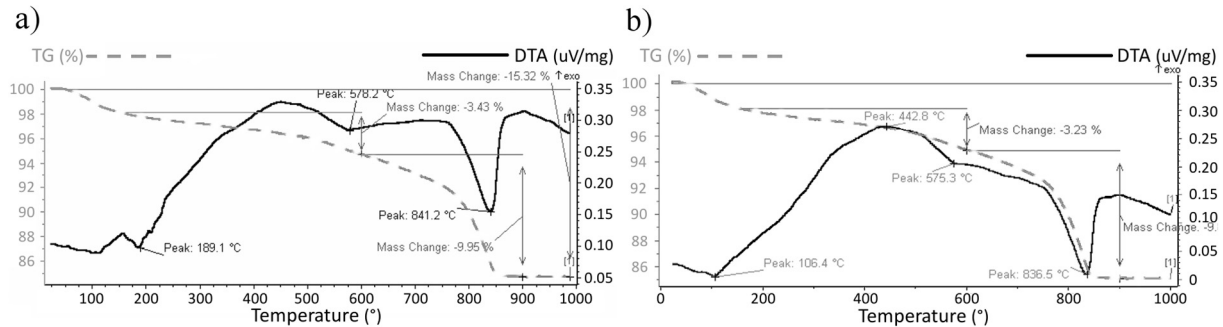


Fig. 13. DTA and TGA of the clayey soil treated with single (a) and double (b) fluid jet grouting.

differences. The DTA curves shows endothermic peaks corresponding respectively to the polymorphic transformation of the quartz (at 578° and 575° for single and double fluid case) and to the decomposition of calcium carbonate (at 836° and 841° for single and double fluid case). The TGA curves also show equal weight losses in the range between the room temperature and $900^\circ C$, most likely due to the decomposition of calcite.

To further clarify the implications of the above results, another experiment was carried out on samples of single and double fluid materials. After removing the outer envelope, two samples extracted from the columns were cut and their intact middle surfaces were painted with a 1% alco-

holic solution of phenolphthalein. When the pH values are lower than 8.2, the painted surfaces show no visible changes of colour, but for pH larger than 9.8, they assume a violet pigmentation (Collepari et al. (2014)). This test showed a meaningful difference between the two materials: the samples treated with single fluid assumed the typical violet coloration (Fig. 14a), while those treated with double fluid remained unchanged (Fig. 14b). This different response of the clay treated with single and double fluid can be thus justified with the different degree of carbonation of the portlandite, $Ca(OH)_2$, one of the cement hydration products. While portlandite is characteristically alkaline, when interacting with CO_2 , calcite ($CaCO_3$) is

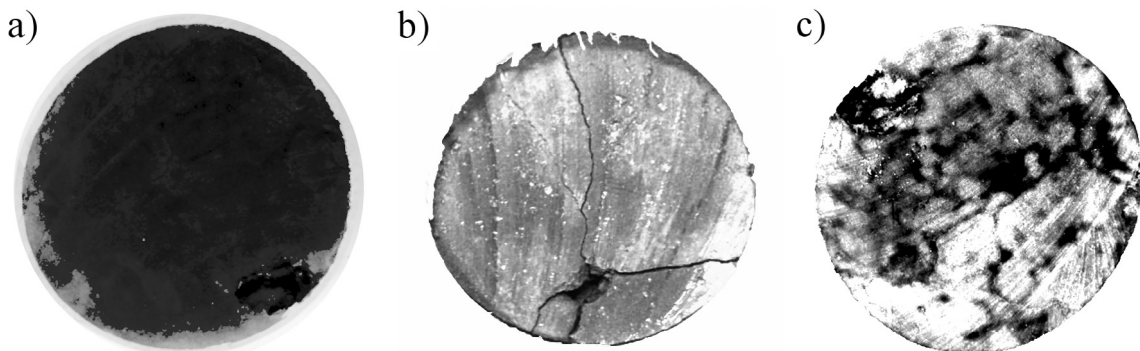


Fig. 14. Results of phenolphthalein test for soil treated with single (a) and double (b) fluid jet grouting and for soil treated with single fluid after 24 h of air exposure (c).

formed, which has lower alkaline characteristics. The lack of violet coloration for the double fluid sample could thus stem from the carbonation of the portlandite activated by the injection of air, whereas the violet coloration of the single fluid sample implies the presence of not yet carbonated portlandite. As further proof, the single fluid sample exposed to air after painting with phenolphthalein tended to lose its violet coloration in a few hours (Fig. 14c). This change can be then ascribed to the carbonation of the small amount of portlandite still present in the single fluid material. In conclusion, the faster carbonation of the double fluid material induced by the insufflation of air rich with CO₂ could have avoided the formation of bigger calcite crystals and thus may be the reason for the lower strength seen in the laboratory tests (Table 4). In fact, it is well known (Jaewd et al., 1978; Ghosh et al., 2002) that cement products are particularly sensitive to the presence of alkaline carbonates as they accelerate the hydration of cement. In this case, these compounds arise from the contact between the newly formed portlandite and cement containing alkali products. The hydration process determined by the carbon dioxide results in poorer mechanical performance than conglomerates cured in absence of CO₂. (e.g. Kakali et al., 2000).

3. Conclusions

The present study focuses on the strength of the material obtained with jet grouting to investigate the effects of two very common versions of the technology: the single and double fluid systems. Two real scale experiments were carried out on site, with single and double fluid jet grouting performed in both sandy and clayey soil deposits. Several samples were cored from the columns and subjected to mechanical tests and to different analytical procedures to compare the composition of the material formed with the two injection systems. The evidence shows that strength is significantly lower for clayey than for sandy soil. This is due the more difficult erosive capacity of the jet in plastic soils that originates because of incomplete mixing between the binding agent and original soil particles.

With a focus on the differences between the single and double fluid system, the two studied cases show the positive role of the air used in the double fluid system to increase the column diameter. As a counterpart, the uniaxial compression strength is always much lower for the double fluid than for the single fluid material.

The analysis performed for the sandy soils identifies the proportion of cement present in the material as the main cause of the observed difference in strength. Uniaxial compressive strength was found to increase with the cement/soil ratio of the material. The lower presence of cement in the double with respect to the single fluid columns was confirmed by SEM, XRD, TGA and DTA analyses, which were carried out to observe the mineralogical composition of the materials. The large differences observed from these tests suggest that other negative effects of the air jet (e.g.

washing of the cement grout from soil particles surfaces) cannot not be excluded. In conclusion, the injection parameters (primarily cement-water ratio and lifting speed of the monitor) should be assigned according to the expected diameter of the column obtainable in each case and by defining a suitable proportion of cement in the obtained material.

To avoid this difference in the field trial performed in clayey soil, a larger amount of cement was injected in the double than in the single fluid system to compensate for the larger dimension of column in the first case. The estimated amount of cement for unit volume of column is thus slightly larger for double than for single fluid. This result is also confirmed by the mineralogical experiments, that reveal a similarly low content of cement in both cases. The lower amount of cement than that in the first field trial can be explained by the difficulty in mixing grout and clayey soils, and also to the lower content of portlandite. Portlandite, Ca(OH)₂, one of the main hydration products of cement, is generally less evident since its Ca⁺⁺ ions deriving from the water dissolution tend to be exchanged with the cations of the clayey soil. However, in spite of their similar compositions, the strength of the double fluid is again much lower than that of the single fluid material. The faster carbonation of the portlandite enhanced by the carbon dioxide (CO₂) insufflated with the air jet may have attributed to this result. This phenomenon induces the formation of micro tensions that reduce the dimension of calcite (CaCO₃) crystals. As a result, while submicrometric crystals are seen from the SEM analyses attached to the clayey particles treated with single fluid jet grouting, the same effect disappears in the double fluid case.

In conclusion, the mechanical and mineralogical tests performed in the two case studies converge to identify a strong relation between injection system and material strength for jet grouting. The differences can be partly explained by the amount of injected cement in relation to the dimension of columns. Other reasons could be found in the different physical or chemical phenomena activated by the injection systems, *i.e.* a possible segregation between soil and grout promoted by the air jet, or in the different carbonation rate of the portlandite due to CO₂ present in the air jet.

The above conclusions, certainly not exhaustive, should be examined further in other contexts, *i.e.* for different soil types, quantities and types of cement, injection systems etc., to understand the relevant mechanisms activated by jet grouting. This kind of analysis cannot be performed uniquely in the laboratory because factors related to the execution of the technology cannot be reproduced. Although affected by a larger complexity and uncertainty in the interpretation of results, site investigations like the ones herein carried out are the only alternative. The results of this investigation represents an opportunity to improve jet grouting technology, optimize its mechanical performances and lead to more rewarding applications.

References

- Atangana Njock, P.G., Shen, J.S., Modoni, G., Arulrajah, A., 2018a. Recent advances in horizontal jet grouting (HJG). *Arab. J. Sci. Eng.* 43, 1543–1560.
- Atangana Njock, P.G., Chen, J., Modoni, G., Arulrajah, A., Kim, J.H., 2018b. A review of jet grouting practice and development. *Arab. J. Geosci.*, 11–459
- Coats, A.W., Redfern, J.P., 1963. Thermogravimetric analysis: a review. *Analyst* 88–1053, 906–924. <https://doi.org/10.1039/AN9638800906>.
- Colleparidi, M., Colleparidi, S., Troli, R., 2014. Il nuovo calcestruzzo. Enco Srl.
- Croce, P., Flora, A., Modoni, G., 2014. *Jet grouting: Technology, Design and Control*. Taylor & Francis Group, ISBN 978-0-415-52640-1.
- Croce, P., Modoni, G., 2007. Design of Jet Grouting Cut-offs, Ground Improvement, Thomas Telford, 11-1, pp. 11–19.
- EN 197-1, 2011, Cement – Part 1: Composition, specifications and conformity criteria for common cements, Technical Committee CEN/TC 51, Cement and building limes.
- Eramo, N., Modoni, G., Arroyo Alvarez de Toledo, M., 2012. Design control and monitoring of a jet grouted excavation bottom plug. In: Viggiani (Ed.), *Proc. of the 7th Int. Symposium on Geotechnical Aspects of Underground Construction in Soft Ground*, TC28 IS Rome. Taylor & Francis Group, London, 16–18 May 2011, pp. 611–618.
- Flora, A., Modoni, G., Lirer, S., Croce, P., 2013. The diameter of single, double and triple fluid jet grouting columns: prediction method and field trial results. *Géotechnique* 63–11, 934–945.
- Flora, A., Modoni, G., Croce, P., Siepi, M., Kummerer, C., 2017. What future for jet grouting? A European perspective. In: *Proc. of the Int. Conf. Grouting 2017*. ASCE library, Honolulu, July 2017, pp. 358–381.
- Ghosh, S.N., 2002. *Advances in Cement Technology: Chemistry, Manufacture and Testing*, second ed. Tech. Books International, New Delhi, India, pp. 687–697.
- Hewlett, P., 2003. *Lea's Chemistry of Cement and Concrete*. Butterworth-Heinemann.
- ICDD, International Centre of Diffraction Data, 2017, <http://www.icdd.com/>.
- Iolli, S., Modoni, G., Chiaro, G., Salvatore, E., 2015. Predictive correlations for the compaction of clean sands. *Transp. Geotech.* 4, 38–49.
- Jaewd, I., Skalny, J., 1978. Alkalies in cement: a review and effects of alkalies on hydration and performance of Portland cement. *Cem. Concr. Res.* 8 (1), 37–51.
- Kakali, G., Tsivilis, S., Aggeli, E., Bati, M., 2000. Hydration products of C3A, C3S and portland cement in the presence of CaCO₃. *Cem. Concr. Res.* 30 (7), 1073–1077.
- Kaushinger, J.L., Perry, E.B., Hankour, R., 1992. Jet grouting: state of the practice. In: *Proc. Grouting, Soil Improvement and Geosynthetics*, vol.1. ASCE, New York, pp. 169–181.
- Kitazume, M., Terashi, M., 2013. *The Deep Mixing Method*. CRC Press, Taylor & Francis group, p. 405.
- Klug, H.P., Alexander, L.E., 1974. *X-Ray Diffraction Procedures: For Polycrystalline and Amorphous Materials*. Wiley.
- Lee, F.H., Lee, Y., Chew, S.H., Yong, K.Y., 2005. Strength and modulus of marine clay-cement mixes. *J. Geotech. Geoenviron. Eng.* 131 (2), 178–186.
- Mackenzie, R.C., 1970. *Differential Thermal Analysis* vol. 1, 479.
- Mascolo, G., Mascolo, M.C., Vitale, A., Marino, O., 2010. Microstructure evolution of lime putty upon aging. *J. Crystal Growth* 312, 2363–2368.
- Miki, G., 1973. Chemical stabilization of sandy soils by grouting in Japan. *Proceedings of the 8th ICSMFE*, pp. 395–405.
- Modoni, G., Croce, P., Mongiovì, L., 2006. Theoretical modelling of jet grouting. *Géotechnique* 56 (5), 335–347.
- Modoni, G., Bzówka, J., 2012. Analysis of foundations reinforced with jet grouting. *J. Geotech. Geoenviron. Eng. ASCE* 138 (12), 1442–1454.
- Modoni, G., Flora, A., Lirer, S., Ochmański, M., Croce, P., 2016a. Design of jet grouted excavation bottom plugs. *J. Geotech. Geoenviron. Eng.: ASCE* 142 (7).
- Modoni, G., Wanik, L., Giovinco, G., Bzówka, J., Leopardi, A., 2016b. Numerical analysis of submerged flows for jet grouting. *Proc. ICE, Ground Improv.* 169 (1), 42–53.
- Ochmański, M., Modoni, G., Bzówka, J., 2015a. Numerical analysis of tunnelling with jet-grouted canopy. *Soils Found.* 55, 929–942.
- Ochmański, M., Modoni, G., Bzówka, J., 2015b. Prediction of the diameter of jet grouting columns with artificial neural networks. *Soils Found.* 55–2, 425–436.
- Qiu, J., Liu, H., Lai, J., Lai, H., 2018. Investigating the long-term settlement of a tunnel built over improved loessial foundation soil using jet grouting technique. *J. Perform. Constructed Facil.*, 32–35
- Reimer, L., 1998. *Scanning Electron Microscopy – Physics of Image Formation and Microanalysis*. Springer.
- Robertson, P.K., 1990. Soil classification using the cone penetration test. *Can. Geotech. J.* 27–1, 151–158.
- Salvatore, E., Modoni, G., Andò, E., Albano, M., Viggiani, G., 2017. Determination of the critical state of granular materials with triaxial tests. *Soils Found.* 57–5, 733–744.
- Shen, S., Wang, Z., Yang, J., Ho, C., 2013. Generalized approach for prediction of jet grout column diameter. *J. Geotech. Geo-Environ. Eng.: ASCE*.
- Taylor, H.F.W., 1997. *Cement Chemistry*. Thomas Telford, p. 548.
- Tinoco, J., Gomes, Correia A., Cortez, P., 2014. Support vector machines applied to uniaxial compressive strength prediction of jet grouting columns. *Comput. Geotech.*, 132–140
- Toraldo, C., Modoni, G., Ochmański, M., Croce, P., 2018. The characteristic strength of jet-grouted material. *Géotechnique* 68 (3), 262–279.
- Van der Stoep, A.E.C., 2001. *Grouting for Pile Foundation Improvement* PhD thesis. Delft University Press, p. 217.
- Wanik, L., 2017. *Influence Analysis of Selected Parameters on Geometrical and Mechanical Properties of Jet Grouting Columns* PhD thesis. Silesian University of Technology, Gliwice (Poland).
- Wanik, L., Mascolo, M.C., Bzówka, J., Modoni, G., Shen, J.S.L., 2017. Experimental evidence on the strength of soil treated with single and double fluid jet grouting. In: *Proc. of the Int. Conf. Grouting 2017*. ASCE library, Honolulu (USA), pp. 52–61.